J Mater Sci (2012) 47:1046–1053
DOI 10.1007/s10853-011-5893-x

Direct fluorination as a novel organophilic modification method for the preparation of Illite/polypropylene nanocomposites

Jinhoon Kim · Euigyung Jeong · Young-Seak Lee

Received: 6 June 2011 / Accepted: 22 August 2011 / Published online: 7 September 2011

Abstract This study reports the application of illite as a clay filler and direct fluorination as an organophilic modification for clays. Illite was also modified using conventional methods, with reagents such as 3-aminopropyltrimethoxysilane and hexadecyl-trimethoxysilane for comparison of the resultant illite/polypropylene (PP) composites with the fluorinated illite/PP composites. The thermal properties, flame retardancy, and mechanical properties of the resultant composites were also investigated. Fluorination of illite resulted in exfoliation and more thermally stable organophilic modification compared with the conventional silane treatment. When comparing two different silane-treated illite/PP composites with fluorinated illite/PP composites, fluorinated illite had better thermal stability and exfoliation after modification and more improved dispersion in PP matrix. This resulted in improved thermal stability, flame retardancy, and mechanical properties compared with the silane-treated illite/PP composites. The fluorinated illite/PP composite exhibited a 28% increase in thermal stability and a 50% increase in flame retardancy compared with neat PP. Fluorination of illite yielded at least 50% further improvement in the thermal stability and flame retardancy of the resulting illite/PP composites compared with the conventional silane treatments.

J. Kim · E. Jeong · Y.-S. Lee (✉)
Department of Fine Chemical Engineering and Applied Chemistry, BK21-E2M, Chungnam National University, Daejeon 305-764, Republic of Korea
e-mail: youngslee@cnu.ac.kr

Introduction

Clay/polymer nanocomposites have been the subject of many studies since the early 1990s because of their outstanding mechanical strength, thermal properties, and flame retardancy [1, 2]. The outstanding properties of clay/polymer composites are attributed to the characteristic properties of clay materials, such as high aspect ratios and excellent thermal properties [3, 4]. Moreover, clays are naturally abundant, cheap, and eco-friendly.

Most of these research efforts have focused on montmorillonite (MMT), a smectite-type clay that expands well in water [5]. However, it has been reported that non-expandable mica clay has the advantage of a higher aspect ratio, which enables researchers to improve the target properties of clay/polymer composites even more compared with smectite clays, such as MMT [6]. Illite is a mica clay, and it is more abundant than MMT, composing of 50% of mineral materials on earth [7]. These characteristics suggest that illite may also be useful for improving certain properties of polymer matrices.

When the clay/polymer composites are prepared, three types of clay/polymer nanocomposites are thermodynamically achievable [8]; (1) intercalated nanocomposites, which feature the insertion of polymers into the layered silicate structure and an increase in interlayer distances of the clay; (2) flocculated nanocomposites, composed of intercalated nanocomposites with flocculated clays resulting from the hydroxylated edge–edge interactions between the clay layers and exhibiting low miscibility with polymers; and (3) exfoliated nanocomposites, in which the individual clay layers are separated in a polymer matrix. Intercalated nanocomposites exhibit improved properties compared with pristine polymers or conventional composites, and exfoliated nanocomposites exhibit similarly or

further improved properties with lower clay loadings [9]. To prepare intercalated or exfoliated nanocomposites, the hydrophilic clay materials are organophilically modified to enhance dispersion in hydrophobic organic polymers with quaternary amine-based surfactants via cation exchange reactions or with silane coupling agents via condensation [10, 11]. However, these methods are time consuming, expensive, and toxic. Moreover, the long alkyl chains of these chemicals decrease the reinforcing effect of the clay and tend to thermally degrade at temperatures in the range of 220–250 °C [12]. In this regard, direct fluorination may be an efficient method to increase the organophilicity of otherwise hydrophilic clay materials quickly and without using chemicals containing long alkyl chains [13]. Moreover, fluorination of fillers often enhances the interfacial adhesion between fillers and polymers and the filler dispersion in a polymer matrix [14, 15].

With this in mind, this study reports the application of illite as a clay filler and fluorination as an organophilic modification method for clays. Illite was also modified using conventional methods, using 3-aminopropyl-trimethoxysilane (APS) and hexadecyl-trimethoxysilane (HDS) to compare the properties of the resultant illite/polypropylene (PP) composites with those of the fluorinated illite/PP composites. Because of the low cationic exchange capacity of illite, conventional cationic exchange modification was not attempted [16]. The thermal properties, flammability, and mechanical properties of the resultant composites were also investigated.

Experimental

Materials

The illite used in this study was purchased from Yong Koong Illite Co. of Korea. Polypropylene homopolymer (H7810) with a melt flow index (MFI) of 1 g/10 min was obtained from LG Chem, Ltd. of Korea. APS and HDS were purchased from Aldrich Co. Fluorine (Messer Grieheim Gmbh, 99.8%) and nitrogen (99.999%) gases were used for the direct fluorination of illite.

Organophilic modification of illite

As shown in Table 1, the modified illite samples were labeled according to the modification methods.

Conventional silane modification

To create the modified illite, 1 g of illite was dispersed in 100 mL of a water/methanol mixture (1:1), and 0.1 g of APS or HDS was dissolved in 100 mL of a water/methanol mixture (1:1) and then added to the illite dispersion. The mixture was stirred for 1 h at 25 °C. The modified illite was collected by filtration, washed with water/ethanol mixture (1:1), filtered, and then dried at 80 °C for 24 h.

Fluorination

Fluorination of illite was performed using a fluorination apparatus consisting of a reactor, a vacuum pump, and gas cylinders connected to a buffer tank. The details of the fluorination apparatus are explained in previous reports [15, 17, 18]. Illite was loaded into a nickel boat in the reactor and degassed at 120 °C for 2 h to remove impurities. The subsequent fluorination was performed out at 25 °C for 10 min at a fluorine pressure of 100 kPa and the illite was degassed to remove unreacted gas after fluorination.

Preparation of illite/PP nanocomposites

To investigate only the effect of the modification methods on the properties of the resultant illite/PP composites, no compatibilizer was added. A twin screw corotating extruder (Haake H-25, model Rheomex PTW 16/25, L/D = 25) was used to prepare PP nanocomposites with 5 wt% of the raw or modified illite at an operating speed of 80 rpm and a temperature between 155 and 185 °C. The illite/PP nanocomposites were pressed into sheet forms (20 cm length × 20 cm width × 3 mm thickness) at 230 °C and 20 MPa for 10 min. The sheets were then cut into suitable test specimen sizes for limiting oxygen index (LOI) and tensile strength tests.

Characterization

Fourier transform infrared spectroscopy (FTIR, Bruker opticsIFS 66/SReflectance_ATR mode, Scans: 64 scans) was used to characterize the changes in chemical composition of illite before and after surface modification. X-ray photoelectron spectroscopy (XPS) spectra of the illite samples were obtained with a MutiLab 2000 spectrophotometer (Thermo Electron Co., England) to investigate the changes in chemical composition of the surfaces before and after surface modification using Al Kα (1485.6 eV) X-rays

Table 1 Sample names and preparation methods

Sample	Surface treatment method
Raw-il	No treatment
APS-il	3-Aminopropyltrimethoxysilane
HDS-il	Hexadecyltrimethoxysilane
F-il	Fluorine gas

with a 14.9-kV anode voltage, a 4.6-A filament current, and 20-mA emission current. All samples were pretreated at 10^{-9} mbar to remove impurities. The XPS survey spectra were obtained with a 50-eV pass energy and a 0.5-eV step size. The core-level spectra were obtained with a 20-eV pass energy and a 0.05-eV step size.

A laser-scattering particle size analyzer (Sympatech GmbH Co., HELOS/RODOS) was used to investigate changes in the particle size of the illite after modification.

X-ray diffraction (XRD) was used to investigate the structural changes of the illite in the nanocomposites. A wide-angle XRD apparatus (Philips PW3040) was operated using Cu Kα radiation with a wavelength of 1.5418 Å at a step size of 0.01° and a scan rate of 0.3°/min.

A thermogravimetric analysis (TGA) was performed to investigate the thermal properties of the illite/PP nanocomposites with a Shimadzu TGA-50H thermoanalyzer at a scan rate of 5 °C/min under nitrogen to evaluate the integral procedure decomposition temperature (IPDT) with a flow rate of 2×10^{-5} m^3/min.

The limiting oxygen index (LOI), defined as the minimum fraction of O_2 in a gas mixture of O_2 and N_2 that would support flaming combustion, was measured using an apparatus (HC-2-type) in accordance with ASTM D2863-77. The specimen size was $100 \times 6.5 \times 3$ mm^3. The bar-type specimen was suspended vertically and ignited using a Bunsen burner. The flame was removed, and a timer was started. The concentration of oxygen was increased when the flame on the specimen was either extinguished before burning for 3 min or 5 cm of the bar had burnt away. The oxygen content was adjusted until the limiting oxygen concentration was determined. LOI data were obtained with five replicates.

The tensile properties of the composites were tested using a universal tester (Housefield Co. Ltd., H10 K–S) in accordance with ASTM D3822. The gauge length was 50 mm, and the strain rate was 2.5 mm/min at RT.

Results and discussion

Chemical and physical changes of illite after modification

The chemical and structural changes of illite after modification were investigated using Fourier transform infrared spectroscopy (FTIR) and the results are shown in Fig. 1. However, only HDS-il exhibited characteristic bands originating from long alky groups of HDS because the thickness of the APS or fluorine layers on the surface of illite after those modifications was insufficient to cause changes in the FTIR spectra. XPS analysis was therefore performed, and the surface chemical compositions of the raw and modified illites are shown in Fig. 2. In the survey spectrum of Raw-il, no C1 s or F1 s peaks are observed. A new C1 s peak from APS or HDS was observed in the spectra of APS-il and HDS-il, and a new F1 s peak introduced by fluorination was observed in the spectrum of F-il. These suggest that illite was successfully modified with both the conventional and fluorination methods. The sizes of the raw and modified illite particles are shown in Table 2. The size of F-il was smaller than the sizes of

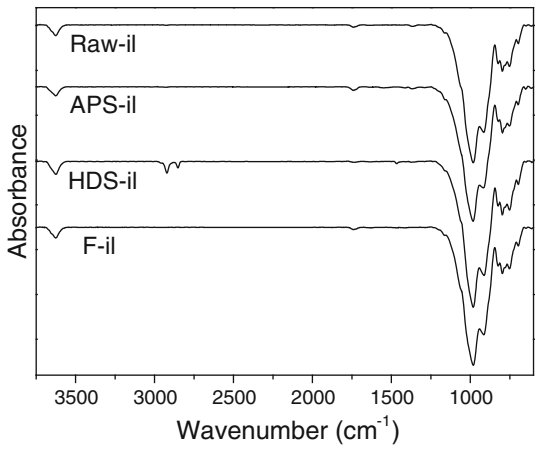

Fig. 1 FTIR survey spectra of the raw and modified illite

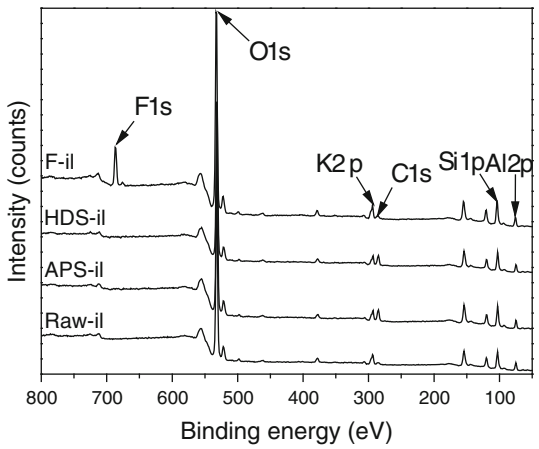

Fig. 2 XPS survey spectra of the raw and modified illite

Table 2 Particles size of illite after different organophilic modifications

Samples	Diameter (μm)		
	x_{10}	x_{50}	x_{90}
Raw-il	1.09	3.71	7.78
APS-il	1.07	3.51	7.54
HDS-il	1.04	3.64	7.67
F-il	0.87	3.21	7.24

Raw-il, APS-il, and HDS-il. In particular, the X_{10} of F-il was approximately 20% smaller than that of Raw-il, whereas those of APS-il and HDS-il were similar to Raw-il. In addition, SEM analysis was also used to investigate the particle size of these illites and the SEM images are shown in Fig. 3. As shown in Table 2, the size of the fluorinated illite particle was significantly decreased, compared to the other samples. It has been reported that the fluorination of MMT-induced exfoliation [13]. Therefore, it seems likely that the particle size of Raw-il was reduced by exfoliation induced by fluorination.

The thermal stabilities of the raw and modified illite samples were compared using TGA, and the results are shown in Fig. 4 Raw-il exhibited gradual thermal degradation, with a weight loss of only 6.2%, even up to 1200 °C. F-il also exhibited gradual thermal degradation and a weight loss similar to Raw-il (6.8%). However, APS-il and HDS-il exhibited faster thermal degradation at approximately 200 °C and greater weight losses of 7.3% (APS-il) and 9.7% (HDS-il). As mentioned earlier, the long alkyl chains of APS and HDS thermally degrade at 200–220 °C [12]. Hence, the greater weight loss observed in APS-il and HDS-il may be attributed to degradation of the long alkyl chains, resulting in thicker layers of silanes on the illite surface. Fluorine attached to the illite surface only degraded by 0.6% and did so at a much higher temperature of ~300 °C. This suggests that a relatively small amount of more thermally stable fluorine was introduced on the illite surface. These differences in the thermal degradation behavior are expected to affect the thermal properties and flammability of the resultant illite/PP composites.

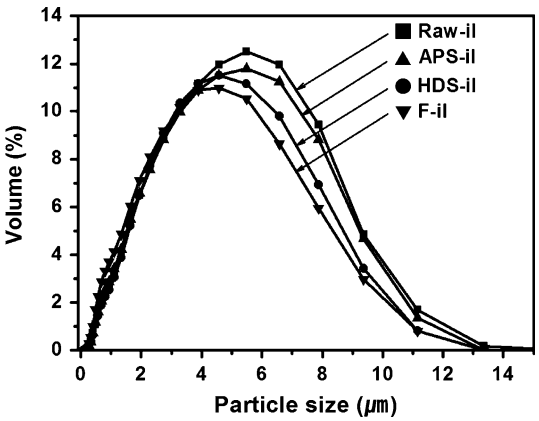

Fig. 3 Particle size distribution of illite

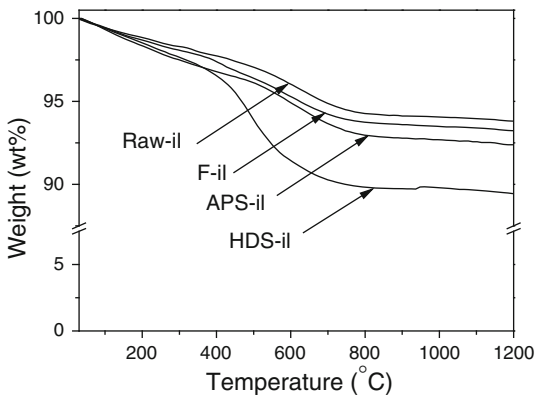

Fig. 4 TGA curves of the raw and modified illite

Illite dispersion in a PP matrix

Figure 5 shows the XRD patterns of the illite/PP composites. Based on the values of 2θ, a layer distance for each illite sample was calculated using Bragg's law, as shown in Eq. 1 [19–21]:

$$d = \lambda/2 \sin \theta \quad (1)$$

where λ is the X-ray wavelength, d is the distance between layers, and θ is the difference between the incident and reflected angles.

The calculated interlayer distances in the raw and modified illite are shown in Table 3. All of the nanocomposite samples exhibited increased illite interlayer distances after organophilic modification. The layer distance in the F-il/PP composite was largest, suggesting that fluorination of illite guides the intercalation of PP into illite better than do the other modification methods, even with

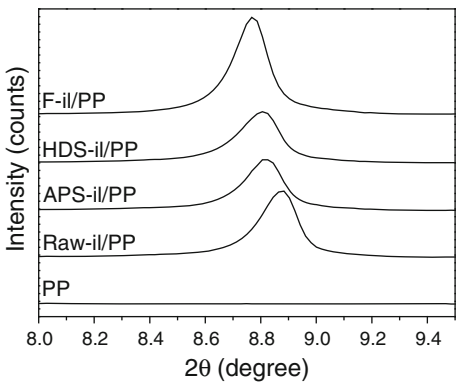

Fig. 5 XRD patterns of the illite/PP composites

Table 3 Distances between layers of the raw and modified illite

Samples	2θ (Peak value)	d (Å)
Raw-il/PP	8.8838	9.942
APS-il/PP	8.8255	10.008
HDS-il/PP	8.8061	10.031
F-il/PP	8.7673	10.074

the smaller size of fluorine compared with the long alkyl chains. However, considering that the increase in the layer distance in clay materials is usually a few nanometers, it seems that very little intercalation occurred in all of the illite composites. This is mainly due to the nonexpandable character of mica-type clays [22–24]. The layers of illite were tightly bound, largely precluding the intercalation of PP into the layers.

Figure 6 depicts the raw and modified illite dispersion in PP polymer matrices. The marked are illite particles in the PP. Raw-il has larger sizes in the PP, whereas the size of the modified illite is relatively small, exhibiting thin needlelike shapes. The thin needlelike shapes appear because the illite itself has layered structures. When the layered illite forms a composite with PP polymer, some exfoliation of the illite occurs. As a result, the illite becomes thin, due to the reduction of the thickness of the layers. This usually increases as the affinity of illite to the PP polymer improves. The hydrophilic raw illite is unlikely to disperse well in the hydrophobic PP matrix. However, the organophilically modified illite exhibits significantly improved affinity for PP, resulting in remarkably improved dispersion in the polymer matrix. Comparing the three modified illites, the order of dispersion is APS-il < HDS-il < F-il. F-il is the most dispersed with almost all of the clay particles forming thin, needlelike shapes without any aggregation. This may be attributed to the synergistic effect induced by fluorination of the illite. As shown earlier, when illite was fluorinated, the size was reduced by exfoliation. In addition, fluorinated illite had more affinity for the hydrophobic polymer matrix than the conventional silane-modified illite. It has been reported that the fluorination of carbon-based materials improves their affinity for organic polymers [13–15, 25, 26]. A similar effect seems to be induced by fluorination of the illite. The increased exfoliation and improved affinity for PP induced by fluorination may synergistically improve the dispersion of illite in the PP matrix. The improved dispersion in particular is expected to improve various properties of the resulting composites.

Thermal properties and flame retardancy of illite/PP nanocomposites

Figure 8 shows TGA and DTG curves for the prepared nanocomposites. The thermal stability of PP improved after the raw and modified illite additions, with higher decomposition temperatures and T_{max} as shown in Fig. 7. Table 4 contains the thermal stability parameters of the composites, such as the initial decomposition temperature (IDT) and the integral procedural decomposition temperature (IPDT), obtained from the TGA and DTG curves. These values allow a quantitative comparison of thermal stabilities of the composite. The IPDT is calculated using the following Eq. 2 [27, 28]:

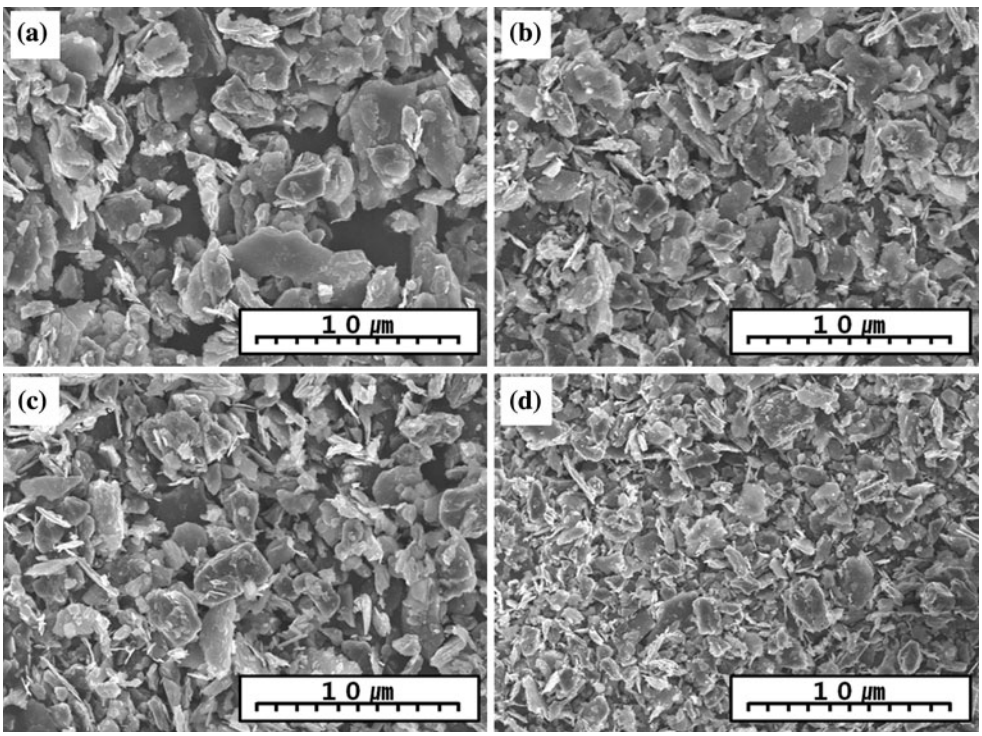

Fig. 6 SEM images of the samples **a** Raw-il, **b** APS-il, **c** HDS-il, **d** F-il/PP

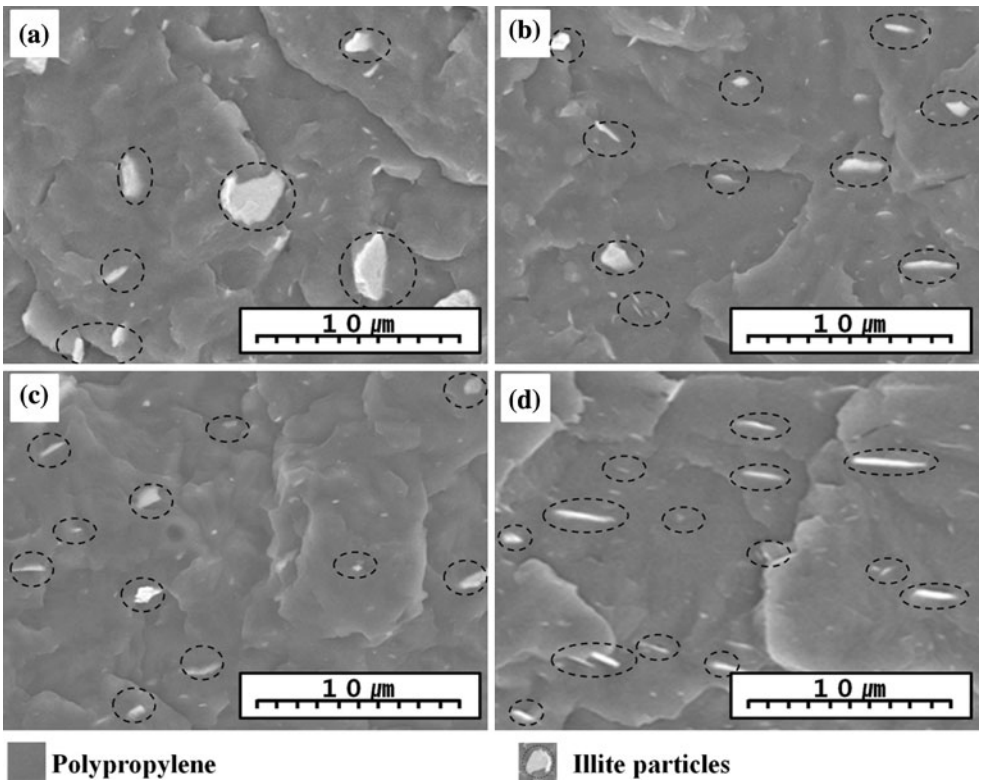

Fig. 7 Dispersion of the illite particles in PP **a** Raw-il/PP, **b** APS-il/PP, **c** HDS-il/PP, **d** F-il/PP

$$\mathrm{IPDT}(^{\circ}\mathrm{C}) = \mathrm{A}^{*}\mathrm{K}^{*}(\mathrm{T_f} - \mathrm{T_i}) + \mathrm{T_i} \quad (2)$$

After the additions of raw or modified illite to PP, the thermal stability of the resulting illite/PP composite improved, showing increased IDPs and IPDTs. Increases of 18.2 and 21.2% were observed for additions of raw illite and neat PP, respectively. The increases in the IDT and IPDT of the modified illite/PP composites occurred in the following order: APS-il/PP (18.8%, 21.7%) < HDS-il/PP (20.9%, 25.6%) < F-il (25.1, 28.1%). This order is the same as the dispersion of the modified illite in the PP matrix. As mentioned earlier, F-il exhibited a remarkable improvement in dispersion in the PP polymer compared with the other modified illite samples. Therefore, the thermal stability of the illite/PP composites is attributed to the dispersion of the illite in the PP polymer.

The flame retardancy of the composites was also examined, and the values obtained for the limiting oxygen index (LOI) are shown in Fig. 9. On one hand, like the dispersion of illite in PP matrix and the thermal stability of the illite/PP composites, the flame retardancy of the F-il/PP composite was improved by 50% compared with that of neat PP. On the other hand, unlike the trend in the dispersion of illite in the PP matrix and the thermal stability of the illite/PP composites, the flame retardancy of HDS-il/PP was less than APS-il/PP. This behavior was attributed to the long alkyl chains present in HDS. As mentioned earlier, HDS-il contains more flammable and thermally unstable long alkyl chains than APS-il. Therefore, addition of HDS-il resulted in less flame retardancy in the composites than APS-il/PP, even with better dispersion.

Mechanical properties of illite/PP nanocomposites

Figure 10 depicts the tensile properties of the illite/PP nanocomposites. When Raw-il was added to PP, the tensile strength of the composite decreased marginally because of the poor dispersion of Raw-il. When HDS-il was added to PP, a 10% decrease in tensile strength was observed. This was ascribed to the long alkyl chains of HDS, which are expected to reduce the tensile strength. Both APS-il and F-il improved the tensile strength of the composite, but F-il/PP showed a greater improvement because of the improved dispersion in the PP polymer. However, the increase in tensile strength was only 4%. This value is very small compared with 20–30% increase observed upon the addition of MMT or even another mica clay, potassium secrite [6]. However, in this study, no compatibilizer was added to enhance intercalation of the polymer or exfoliation of the clay in order to separate the effects of the organophilic modification method. Improved tensile strength remains still important and may be further improved by the use of a compatibilizer.

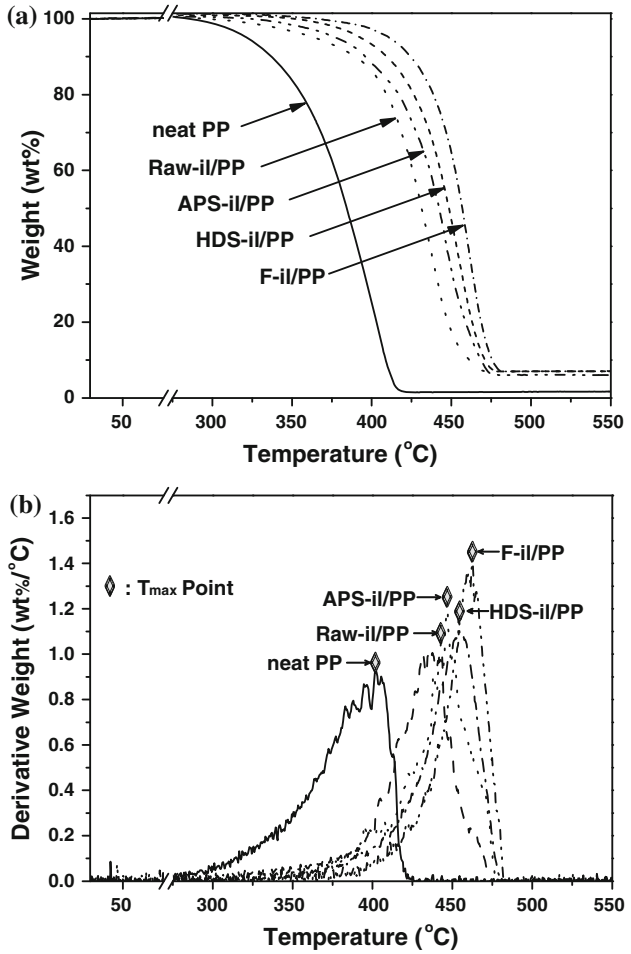

Fig. 8 TGA and DTG curves of the illite/PP composites

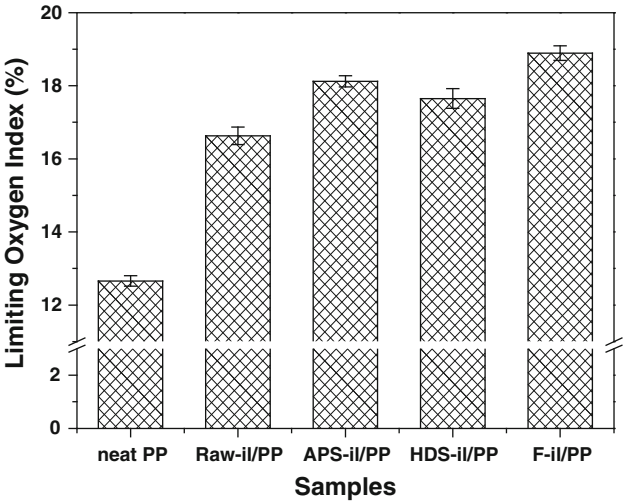

Fig. 9 Flame retardancy of the illite/PP composites

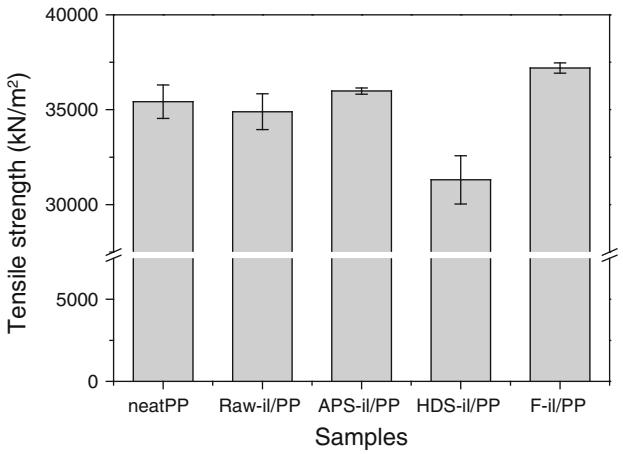

Fig. 10 Tensile strength of the illite/PP composites

Table 4 Thermal stability parameters of the illite/PP composites

	IDT(°C)	ΔIDT(°C)	IPDT(°C)	ΔIPDT(°C)
PP	335	0	391	0
Raw-il/PP	396	61	474	83
APS-il/PP	398	63	476	85
HDS-il/PP	405	70	491	100
F-il/PP	419	84	501	110

IPDT integral procedural decomposition temperature, calculated using Doyle's equation

IPDT (°C) $= A^* \cdot K^* \cdot (T_f - T_i) + T_i$, A^* is the total curve area normalized with respect to both residual weight and temperature, K^* the index of thermal stability, T_f is the final experimental temperature (550 °C), and T_i is the initial experimental temperature (30 °C)

Conclusions

Illite, a mica type clay, was modified using conventional silane treatments or direct fluorination, and modified illite/PP composites were prepared. The fluorination of illite resulted in exfoliation of the clay and a more thermally stable organophilic modification compared with the conventional silane treatments. When comparing two different silane-treated illite/PP composites with the fluorinated illite/PP composites, the fluorinated illite had better thermal stability and dispersion in a PP matrix, resulting in improved thermal stability, flame retardancy, and mechanical properties than the silane-treated illite/PP composites. However, the illite/PP composites exhibited little polymer intercalation and clay exfoliation, resulting in little improvement in the mechanical properties of the composites. This is attributed to strong interactions between illite layers, which often hinder the use of clays for the composites. It should be noted that this study did not use any compatibilizer in order to focus on the effect of the different surface treatments. Hence, it is expected that more intercalation and exfoliation will occur when the

composite is prepared with a compatibilizer. Even though the advantage of illite as a clay filler for layered silicate/polymer nanocomposites may not be immediately clear from these results, it is still noteworthy that the direct fluorination of clay may be a more efficient modification method than other conventional organophilic modification methods.

References

1. Kiliaris P, Papaspyrides CD (2010) Prog Polym Sci 35:902
2. Suprakas SR, Masami O (2003) Prog Polym Sci 28:1539
3. Garcés JM, Moll DJ, Bicerano J, Fibiger R, McLeod DG (2000) Adv Mater 12:1835
4. Lee SK, Bai BC, Im JS, In SJ, Lee Y-S (2010) J Ind Eng Chem 16:891
5. Shanmugharaj AM, Rhee KY, Ryu SH (2006) J Colloid Interface Sci 298:854
6. Uno H, Tamura K, Yamada H, Umeyama K, Hatta T (2009) Moriyoshi Y Appl Clay Sci 46:81
7. Jeong E, Lim JW, Seo KW, In SJ, Lee YS (2011) J Ind Eng Chem 17:77
8. Ray SS, Okamoto K, Okamoto M (2003) Macromolecules 36:2355
9. Palza H, Vergara R, Yazdani-Pedram M, Quijada R (2009) J Appl Polym Sci 112:1278
10. Sánchez-Martín MJ, Dorado MC, Hoyo CD, Rodríguez-Cruz MS (2008) J Hazard Mater 150:115
11. Park SJ, Kim BJ, Seo DI, Rhee KY, Lyu YY (2009) Mater Sci Eng A 526:74
12. Golebiewski J, Galeski A (2007) Compos Sci Technol 67:3442
13. Im JS, Lee SK, In SJ, Lee YS (2010) J Anal Appl Pyrolysis 89:225
14. Im JS, Park IJ, In SJ, Kim T, Lee YS (2009) J Fluor Chem 130:1111
15. Im JS, Jeong E, In SJ, Lee YS (2010) Compos Sci Technol 70:763
16. Mitchell JK (1993) Fundamentals of soil behavior, 2nd edn. John Wiley and Sons, Inc., New York ISBN 3-437
17. Yun J, Im JS, Lee YS, Kim HI (2010) Eur Polym J 46:900
18. Lee YS (2007) J Fluor Chem 128:392
19. Sudhakara P, Kannan P, Obireddy K, Rajulu AV (2011) J Mater Sci 46:2778. doi:10.1007/s10853-010-5152-6
20. Kim SJ, Yun SM, Lee YS (2010) J Ind Eng Chem 16:273
21. Ganguly A, Bhowmick AK (2009) J Mater Sci 44:903. doi:10.1007/s10853-008-3183-z
22. Wattanasiriwech D, Wattanasiriwech S (2011) J Eur Ceram Soc 31:1371
23. Wattansiriwech D, Srijan K, Wattanasiriwech S (2009) Appl Clay Sci 43:57
24. Michael AV (1992) Am J Sci 292:58
25. Im JS, Lee YS, Kim JG (2009) Carbon 47:2640
26. Maity J, Jacob C, Das CK, Alam S, Singh RP (2008) Compos Part A 39:825
27. Doyle CD (1961) Anal Chem 33:77
28. Guo B, Jia D, Cai C (2004) Eur Polym J 40:1743